Desalination and Water Treatment
www.deswater.com

doi: 10.5004/dwt.2018.22240

113 (2018) 148–159
May

Recycling of alum sludge for alpha Al_2O_3 production using different chemical treatments

R.M. Khattab, H.A. Badr, H.H. Abo-Almaged*, H.E.H. Sadek

Refractories, Ceramics and Building Materials Department, National Research Centre (NRC), Dokki, 12622 Cairo, Egypt, email: rihamkhattab78@yahoo.com (R.M. Khattab), hayamelassal@yahoo.com (H.A. Badr), Tel. +00201015892223, email: hanan-202@hotmail.com (H.H. Abo-Almaged), hsadek2004@yahoo.com (H.E.H. Sadek)

Received 19 September 2017; Accepted 19 March 2018

ABSTRACT

The present work focused on recycling the alum sludge which is one of the serious problems during the production of potable water. In this work, the alumina was extracted from alum sludge by using different chemical treatment methods after subjecting to different thermal treatments. XRD, XRF, SEM, TEM, IR and surface area measurements were used to detect the properties of the obtained alumina. Alpha alumina was obtained at 1400°C after treatment by NaOH followed by ammonium acetate as a precipitating agent for $Al(OH)_3$ or by direct addition of NH_4OH in one step method at pH 5.5–6. On the contrary, the treatment by NaOH followed by $NaHCO_3$ for precipitation of $Al(OH)_3$ led to the formation of sodium aluminate beside low percentage of alpha alumina after the heat treatment.

Keywords: Wastewater; Water treatment sludge; Alum sludge; Chemical treatment methods; Alumina

1. Introduction

Alum sludge is a waste material referred as alum derived from water treatment sludge. It is produced as a byproduct during the water treatment by alum [1–6]. Alum is used as a coagulant for the organic matter, as an adsorbent to remove phosphorus and heavy metals like Pb(II), Cr(III), Cr(VI), As(III) and As(V) [10] and as a clarifier for the turbidity and color from the drinking water by the hydrolysis of aluminum in the form of glutinous precipitate of aluminum hydroxide [7–15].

The mechanism of alum addition to water can be illustrated as follows; the aluminum in alum is an excellent coagulant in water due to its high charge. When the alum is added to the water, a number of hydrolysis species occurs such as the formation of $Al(OH)^{2+}$, $Al(OH)_2^{+}$, $Al(OH)_3$ and $Al(OH)^{-}_4$, that depends on the pH to remove the particles from the water [16]. The free Al^{3+} ions are hydrated to form highly charged species such as $Al_8(OH)_{20}^{4+}$ that attracts the negatively charged species like clay and $CaCO_3$. These coagulated particles are stuck to the surface of $Al(OH)_3$ as a gel precipitate from the solution, then the clarification of water occurs by the filtration process [16].

The alum sludge is liquid or solid mainly consists of aluminum compounds, SiO_2 and Fe_2O_3. The quantity of this sludge is rather high and it should be handled through recovery of alumina and iron oxide from the sludge as a secondary raw material to be possibly used in production of cements, pigments and ceramics [8].

Alumina (Al_2O_3) is considered as one of the most important ceramic materials due to its numerous applications and varied physical and mechanical properties. It is used for example as a catalyst support, a cutting-tool material, a furnace lining due to its high thermal stability and as a protective barrier against corrosion on alumina-forming alloys. Alumina exists in a variety of metastable structures such as gamma, delta, eta, theta, and chi-alumina as well as a stable form of α-Al_2O_3 phase [17,18].

Many methods have been used for production of alumina powders like sol-gel process, hydrothermal, mechanical milling, co-precipitation, vapor phase reaction, and combustion method [19–26]. These methods depend on utilizing salt or organo materials of alumina compounds for alumina extraction and heat treatment to validate the

*Corresponding author.

1944-3994 / 1944-3986 © 2018 Desalination Publications. All rights reserved.

alumina phase transition occurrence, i.e., gamma, delta, theta, and alpha alumina.

Most of the research areas in recycling of alum or wastes (like aluminum dross) to produce alumina depend on utilizing NaOH and sodium acetate to form double layer hydroxide, and/or applied heat treatment up to 1000ºC to form gamma alumina [8,27]. However, the using ammonium acetate instead of sodium acetate as a precipitating agent to produce the aluminum hydroxide, followed by studying the effect of the thermal treatment at high temperature up to 1400ºC to form alpha alumina is rarely studied. Moreover, the effect of ammonium hydroxide as a precipitating agent instead of NaOH/sodium acetate to produce aluminum hydroxide after adjusting the pH followed by thermal treatment is studied in this research and compared with the other mentioned methods above.

This work will be focused on treatment of the alum sludge by different chemical treatment methods combined with thermal treatment methods. The effect of these methods on the purity of the obtained alumina is studied to produce alpha alumina which has a large marketplace.

2. Material and methods

Alum sludge had been collected from the El Manial water station (Gizza, Egypt) and analyzed by X-ray fluorescence (XRF) as seen in Table 1. The alum slugde is treated by water suction pump to remove the water followed by drying the slurries at 110ºC.

Three chemical treatment methods (as seen in scheme 1) had been utilized depending on pH to determine the amount of the final produced alumina after firing at different temperatures. Moreover, these studies are concerned with estimating the effect of heat treatment on the purity of the produced alumina.

2.1. The first chemical treatment method

This method based on utilizing NaOH and $NaHCO_3$ as starting materials to optimize the pH for precipitating aluminum hydroxide. The utilization of alum sludge procedure to produce $Al(OH)_3$ was illustrated as follows; 10 g of alum sludge, 15 mL of conc. sulfuric acid solution (7 mol/L) and 50 mL distilled water was added into a 500 mL flask with a magnetic stirrer and a temperature controller. The reactants were stirred by a mechanical agitator at a rate of 300 rpm and heated at 170°C for 1 h. After that, 100 mL of distilled water was added into the flask and remained at room temperature overnight to extract soluble compounds from the resulting mixture. Next, the slurry was filtered and sodium hydroxide solution (7.66 mol/L) was slowly added to the filtrate with a constant rate (3 mL/min) under a continuous stirring until pH 12.

Table 1
Chemical analysis of alum sludge by X-ray fluorescence (XRF)

Main constituents	Wt %
SiO_2	35.36
TiO_2	0.82
Al_2O_3	22.38
Fe_2O_3	6.13
MgO	0.88
CaO	3.00
Na_2O	0.35
K_2O	0.47
P_2O_5	0.47
SO_3	1.06
Cl	0.28
LOI	28.43

The flask was retained at room temperature over night for complete separation of $Fe(OH)_3$ from soluble Al compounds and then the resulting slurry was filtrated. The produced solid components with reddish brown color were dried at 100°C for 24 h in an oven after a good washing with distilled water. At this step the filtrate was subjected to two different chemical methods, which are; (1) $NaHCO_3$ solution (0.430 mol/L) was dropped with a constant rate of 3 mL/min to the filtrate to reach pH7. However, in this step, the maximum pH reached 8.5 for the precipitation formation, then the decreasing below pH 8.5 was not happening (this is may be due to the combination of $Al(OH)_3$ precipitate with other salts which may affect on the pH). In general, the solubility of $Al(OH)_3$ is low between pH 4 and pH 9.5 according to previous work [28]. After that, the obtained precipitate was washed with water and was leaved overnight. (2) The other method was depending on the addition of $NaHCO_3$ solution (0.430 mol/L) at 70°C with constant rate 3 mL/min to the filtrate, and then the obtained precipitate was washed with hot water to dissolve the formed salts. Finally, all the powders were dried at 110°C and fired at different temperatures from 600° to 1400°C to optimize the alumina production.

2.2. The second chemical treatment method

The second chemical treatment method based on utilizing NaOH and ammonium acetate as starting materials to optimize the pH for the precipitation of aluminum hydroxide.

In this method, the sludge was treated by H_2SO_4 as the above previous method and then the filtrate was adjusted by 2.2 mol/L ammonium acetate with a constant rate of 3 mL/min at 70°C to re-precipitate $Al(OH)_3$ at pH 8 after extraction of $Fe(OH)_3$ with NaOH, The obtained powders were calcined at different temperatures depending on the X-ray diffraction (XRD) results.

2.3. The third chemical treatment method

This method based on utilizing ammonium hydroxide as starting material to optimize the pH for precipitation of aluminum hydroxide.

In this procedure the waste was treated with H_2SO_4 as the above methods. The obtained filtrate was transferred into the separating conical flask, and then an aqueous ammonium hydroxide was dropwise. It was observed a buff precipitate formed at about pH 5.5–6 like [29,30]. Above

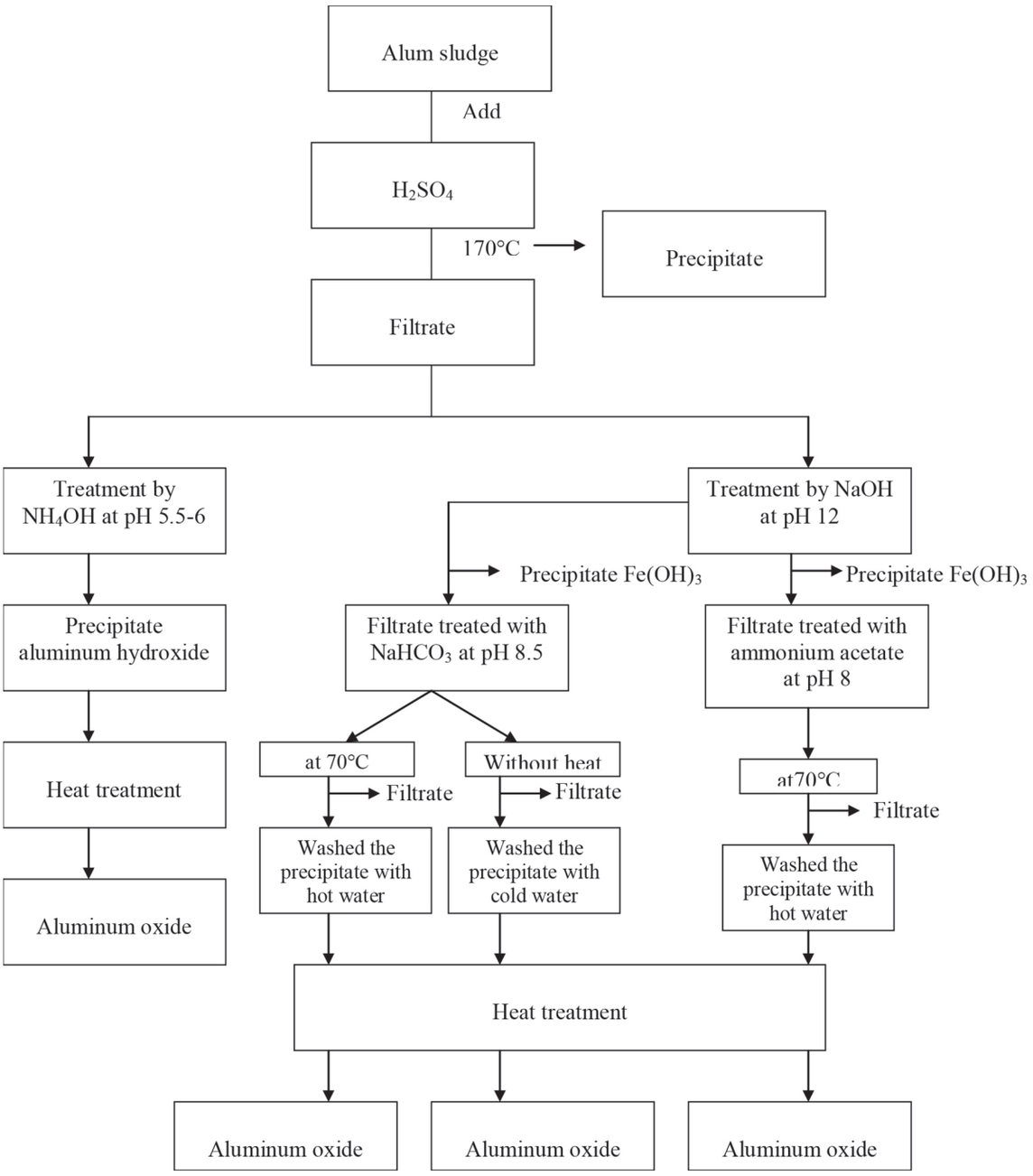

Fig. 1. Flow chart of different chemical treatment method on alum sludge for alumina production.

the pH 6, the color of the precipitation changed to orange color due to the highly extracted $Fe(OH)_3$ with aluminum hydroxide. Thus the pH 5.5–6 was selected to collect the 95% Al_2O_3 from the sludge with minimum amount of Fe_2O_3 as illustrated latter by the XRD and EDAX results. The obtained precipitate was washed with hot water and calcined at different temperatures according to XRD results.

The microscopic images of the samples were taken with a scanning electron microscope (SEM) model FEI, QUANTA FEG, 250. X-ray diffractometer (XRD) (EMPYREAN by Cu Ka radiation with a wavelength of 1.54°A) was used to identify the crystalline phases. Transmission electron microscope (TEM) model JEOL JEM-2100 equipped with a high-angle, angular dark-field detector and an x-ray energy-dispersive spectroscopy system was used to examine the particle size and the degree of crystallinity. Furthermore, Fourier transform infrared spectroscopy (FT-IR, MB154S, and Bomem) was used to determine the main bonds in the powder and the effect of heat treatment on the spectra of alumina structure. The decomposition of the prepared

powders produced after heat treatment was determined by thermogravimetric analysis (DTA & TGA, Setaram Labsy TM TG-DSC16 system). The surface area was calculated according to the Brunauer–Emmett–Teller method (BET) using BEL JAPAN, INC equipment. In this test 0.1 g sample was heated at 300ºC for 3 h under 10–2 vacuum pressure before measurement.

3. Results and discussion

3.1. For the precipitate obtained by NaOH and $NaHCO_3$ and washed with ambient water

3.1.1. XRD analysis

XRD patterns of the prepared and calcined powders are indicated in Fig. 2. The reaction mechanism during the precipitation of aluminum hydroxide [8] is illustrated as follows: first, the aluminum and iron were extracted from alum sludge by acid treatment (H_2SO_4) in the form of soluble sulfates. Then the precipitation of ferric hydroxide was achieved after the addition of NaOH and adjusting the pH at 12, followed by the separation of ferric hydroxide through the dissolution of aluminum hydroxide. Finally the re-precipitation of aluminum hydroxide was achieved after the addition of $NaHCO_3$ and washed with ambient water.

The XRD patterns for the prepared samples show the formation of boehmite (AlOOH) (Fig. 2a) which converts to gamma alumina (γ-Al_2O_3) after calcination at 600°, 800° and 1000°C (Figs. 2b–2d). These results can be explained according to other previous works which indicate the increase in the calcination temperature accompanied with series of transformations; AlOOH → γ-Al_2O_3 → δ-Al_2O_3 → θ-Al_2O_3 → α-Al_2O_3 [31–33]. All alumina phases that produced at low temperatures transformed into α-Al_2O_3 at high temperatures. The transformations from γ phase ended to θ phase need low activation energies, while α transformation proceeds through nucleation, growth and elevated temperature [31–34]. For the powders calcined at 1200°, the XRD patterns (Figs. 2e, 2f) show the formation of θ-Al_2O_3, α-Al_2O_3, $NaAl(OH)_2CO_3$ and $NaAlO_2$ Phases. The appearing of sodium aluminate after calcination at 1200° is attributed to the formation of $NaAl(OH)_2CO_3$ complex during the preparation step. $NaAl(OH)_2CO_3$ complex is mostly transfered into sodium aluminate at high temperature, especially at 1400°C , which affected on the amount of α-Al_2O_3 phase . In general, this complex appeared in an amorphous state at low temperatures that converted into a crystalline state above 1000°C [35].

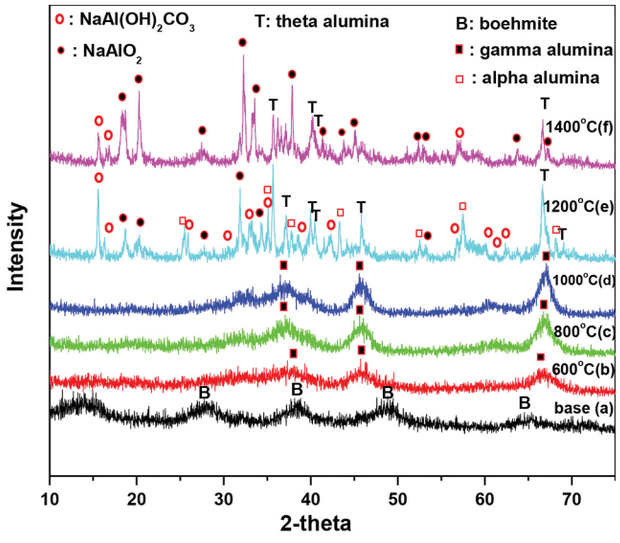

Fig. 2. XRD analysis of the prepared and calcined powders obtained by NaOH and $NaHCO_3$.

3.1.2. SEM analysis

Scanning electron microscope for the precipitated powders at room temperature were washed by ambient water, then calcined at different firing temperatures; 600°, 800°, 1000°, 1200° and 1400°C are shown in Fig. 3. The change in morphology and the size of the powders after calcination are observed with increasing the firing temperature. For powders fired at low temperatures (up to 1000°C), the aggregation of nanoparticles into micro particles was observed. For the sample fired at 1200°C, the powders have some particles with size greater than one micron. Moreover, it is found that the agglomeration decreases with calcination. For powder fired at 1200°C, the transformation of θ-alumina to hexagonal plate α-alumina is investigated. The θ particles have irregular outlines and agglomerate in small particles. Moreover, the samples calcined at 1400°C contain a new phase in rod shape (light gray) refereed to sodium aluminate phase. This is due to the reaction between Al_2O_3 and Na_2O at high temperature in the matrix of the θ-alumina [35].

3.1.3. TEM analysis

The surface morphology by TEM is shown in Fig. 4 for powder precipitated at room temperature and washed with ambient water and calcined at different temperature up to 1400°C. This figure shows that spheroid agglomerates are due to their high surface area at low calcined temperatures up to 1000°C [36]. For the powder calcined at 1200°C, it appears that θ-Al_2O_3 crystallized to α-Al_2O_3 nucleus in hexagonal symmetry. According to another previous work, the critical size for transformation of θ-crystallite to α-crystallite is about ~17 nm [37]. Upon calcination at 1400°C, the TEM image indicates that the retransformation of the formed α-Al_2O_3 to sodium aluminate occurs. The crystallinity and crystallography of the product are proven by selected area electron diffraction (SAED). The SAED shows that the increase of calcination temperature increases the degree and size of crystallizations.

3.1.4. IR analysis

The FTIR spectra of prepared powders washed with water and calcined at different temperatures: 600°, 800°, 1000°, 1200° and 1400°C are shown in Fig. 5.

The spectra of prepared powders show that the characteristic bands of aluminum oxide hydroxide (boehmite) occur at 3423, 2920, 1641, 1104, 905, 705 and 553 cm^{-1} [38].

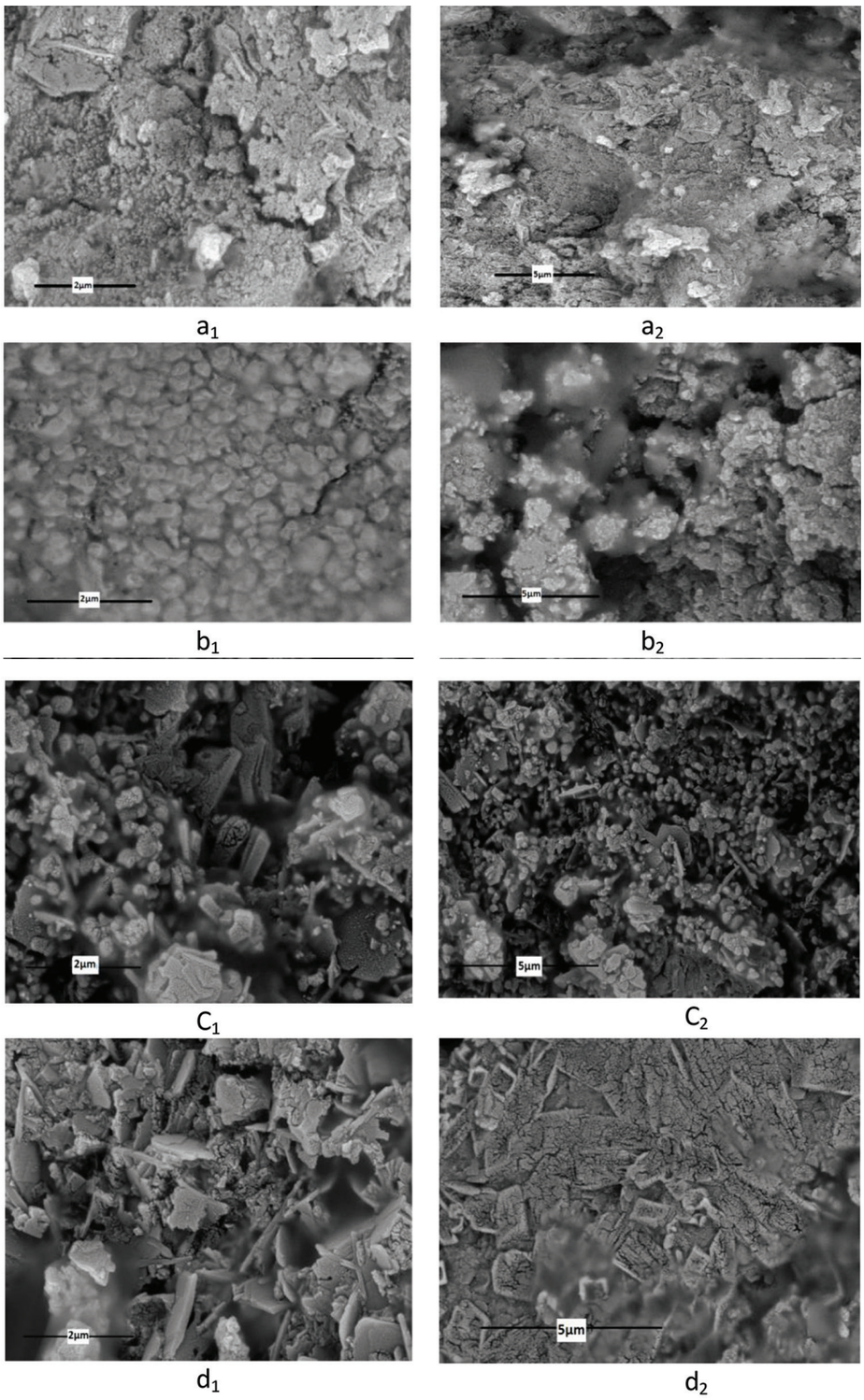

Fig. 3. SEM for the prepared and calcined powders obtained by NaOH and $NaHCO_3$; a: 600°C, b: 800°C, c: 1000°C, d: 1200°C and e: 1400°C.

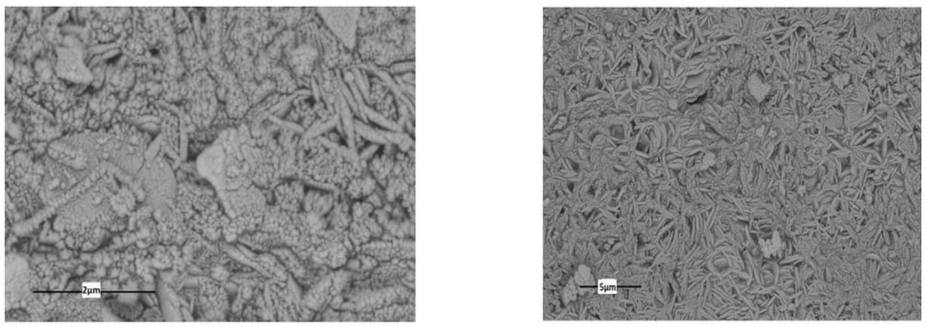

Fig. 3. (Continued).

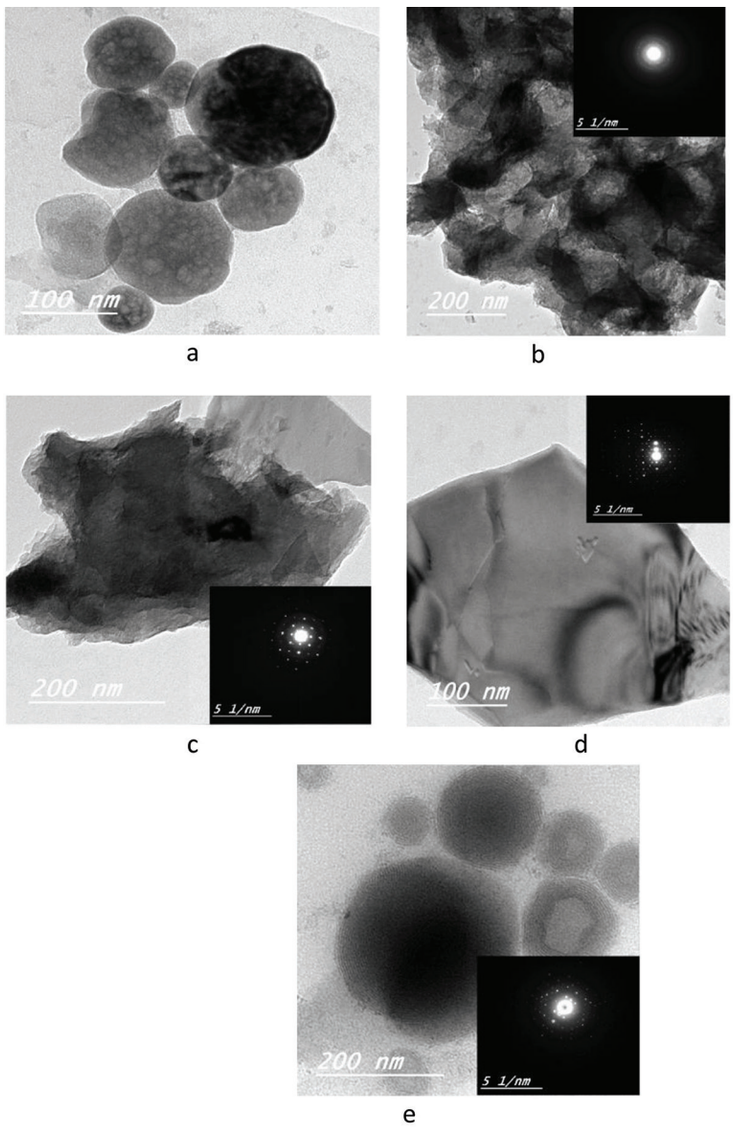

Fig. 4. TEM for the prepared and calcined powders obtained by NaOH and $NaHCO_3$; a: 600°C, b: 800°C, c: 1000°C, d: 1200°C and e: 1400°C.

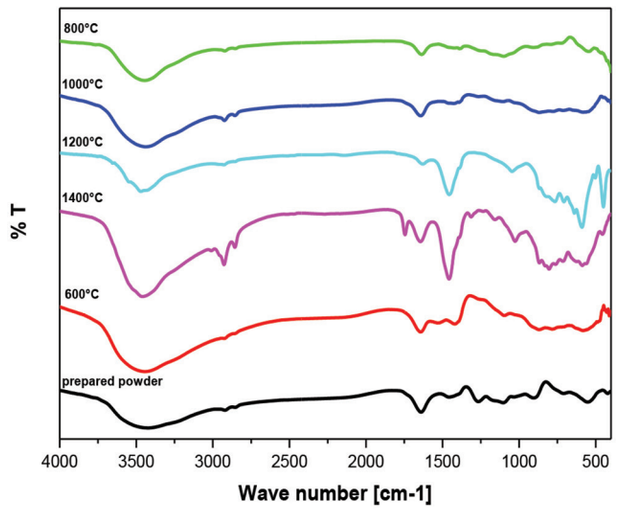

Fig. 5. FTIR spectra of prepared powders by NaOH and $NaHCO_3$ and calcined at different temperatures.

The band observed at 1455 cm^{-1} is assigned to the stretching vibrations of the CO_3^{2-} ion, which confirming the formation of $NaAl(OH)_2CO_3$ complex [35].

Powders calcined at 600°, 800° and 1000°C show the appearance of γ-Al_2O_3. The broad band corresponding to the stretching vibration of Al-O appear from 869 to 487 cm^{-1} for calcined powders at 600°C, from 907 to 546 cm^{-1} for calcined powders at 800°C and from 868 to 581 cm^{-1} for calcined powders at 1000°C [39]. Carbonate bands appear at 1400–1420 cm^{-1} and the intensity decreases with increasing the calcination temperatures.

Bands for α-Al_2O_3 appear at 639, 589 and 449 cm^{-1} for powders calcined at 1200°C and at 622, 588 and 455 cm^{-1} for powders calcined at 1400°C representing stretching vibration of Al-O. While, bands around 707, 1046 and 713, 1025 cm^{-1} are assigned to the symmetric bending of Al–O for calcined powders at 1200° and 1400°C, respectively [40]. From these results, it was observed that the bands intensity of the alpha alumina at 1200°C are high compared with the calcined samples at 1400°C as confirmed by XRD results. The main bands corresponding to the presence of θ-Al_2O_3 appear at 766, 825 cm^{-1} for calcined powders at 1200°C and at 762, 804 cm^{-1} for calcined powders at 1400°C [40]. Peaks represent sodium aluminate, for powder calcined at 1200°C; appear at 505, 707 and 1048 cm^{-1} and at 563, 713 and 1025 cm^{-1} for calcined powder at 1400°C [35].

3.1.5. BET analysis

The BET surface area for samples washed with water and calcined at different temperatures from 600° to 1400°C is shown in Table 2. It was observed that BET surface area decreases with increasing the heat treatments.

3.1.6. TG analysis

TG analysis of the prepared powder washed by ambient water is shown in Fig. 6. It is observed that there are two

Table 2
The BET surface area for samples washed with water and calcined at different temperatures

BET measurement (m^2g^{-1})	Temperature (°C)
1.8141 E^{+02}	600
1.2968 E^{+01}	800
1.0505 E^{+01}	1000
1.4140 E^{+01}	1200
6.9847 E^{+00}	1400

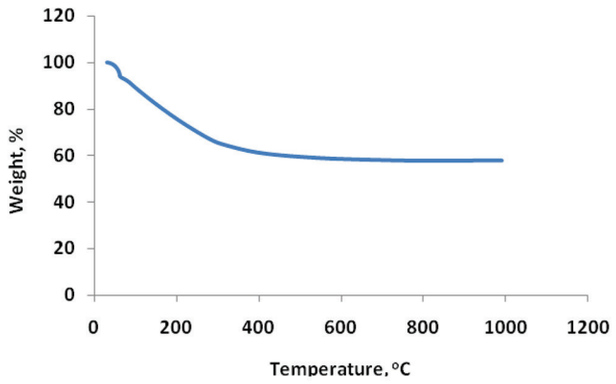

Fig. 6. TG analysis of the prepared powder.

weight loss areas. The first area accompanied by weight loss of about 7.08%. This is related to the destruction of the boehmite structure. On the other hand, the $Al(OH)_3$ obtained in the water was converted to Al_2O_3 by releasing water molecules from the skeletal structure of the $Al(OH)_3$ accompanied by the second weight loss area of about 35%. Finally, the phase transition of γ-alumina, θ-alumina, and a mixture of θ- and α-Al_2O_3 occurred without weight loss as seen in Fig. 6.

3.2. For the precipitate washed by hot water

The results that obtained in the first case washed with ambient water showed a decrease in the formation of α-Al_2O_3 phase after sintering at 1000°C. Accordingly, we used the hot water for washing the precipitate based on utilizing three methods for alumina precipitation:

1. NaOH and $NaHCO_3$ (CP powders)
2. NaOH and ammonium acetate (AC powders)
3. Ammonium hydroxide (AH powders)

The obtained powders were calcined at 1000° to 1400°C.

3.2.1. XRD analysis

XRD analyses for the CP, AH and AC powders prepared in hot condition and calcined at different temperatures are shown in Figs. 7–9, respectively. It is observed that all

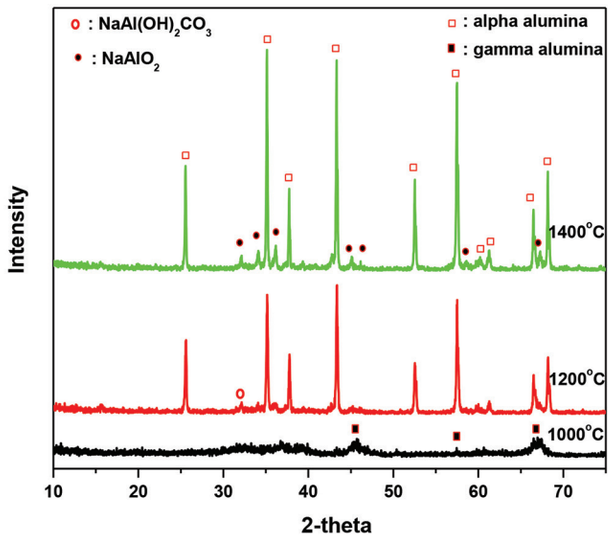

Fig. 7. XRD analysis of the calcined powders (CP) prepared in the hot condition and calcined at different temperatures.

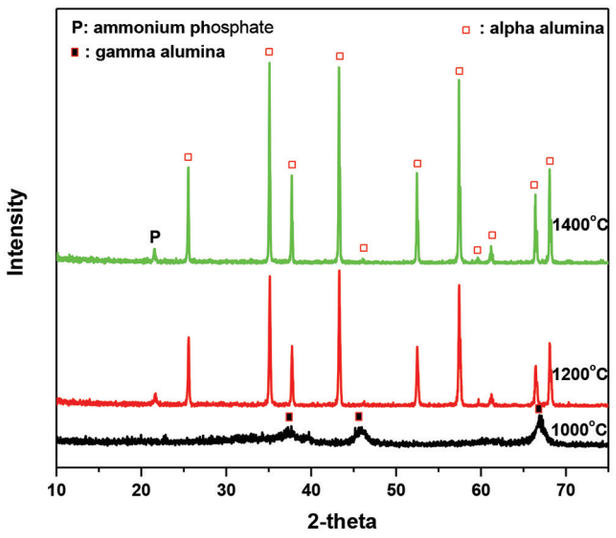

Fig. 8. XRD analysis of the calcined powders (AH) prepared in the hot condition and calcined at different temperatures.

alumina phases produced at low temperature (1000°C) transform to α-Al_2O_3 at high temperatures for all the produced powders (1200° and 1400°C). However, CP and AH show some impurities accompanying with alumina; sodium aluminate and $NaAl(OH)_2CO_3$ (Fig. 7) for CP and aluminium phosphate or iron phosphate for AH (Fig. 8) after calcination at high temperature. As seen from Fig. 7, the amount of sodium aluminate increases and $NaAl(OH)_2CO_3$ decreases with increasing the calcined temperature at 1400°C. The appearing of aluminum phosphate for AH powder (Fig. 8) is due to its adsorption on the surface of Al_2O_3 at pH 5, which is soluble above pH 6.7–7 as shown in the following equations [41,42]:

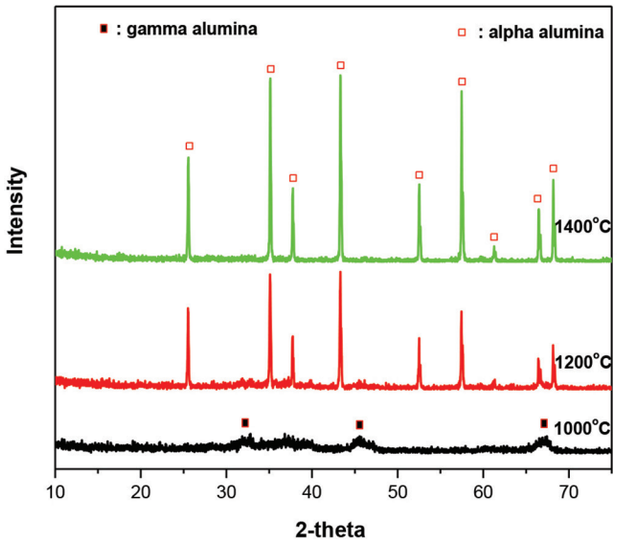

Fig. 9. XRD analysis of the calcined powders (AC) prepared in the hot condition and calcined at different temperatures.

$$Al_2O_3+3H_2O \rightarrow 2Al(OH)_3$$

$$Al(OH)_3+H_2PO_4^- \rightarrow AlPO_4+ OH^-+ 2H_2O$$

For AC powders, the pure corundum phase appears with absence of impurities for other phases as shown in Fig. 9. This result indicates that the utilization of ammonium acetate as a source for aluminum hydroxide precipitation (AC powder) causes reducing of the sodium content in the system compared with utilization of sodium bicarbonate as a source for the formation of aluminum hydroxide (CP powder). Reducing of sodium content during the preparation facilitates the solubility of the formed sodium carbonate salt. Therefore the addition of ammonium acetate leads to the formation of pure corundum without super saturation of sodium carbonate salt during the preparation as done for CP powders.

3.2.2. SEM analysis

SEM images were carried out for the powder calcined at 1400°C as shown in Fig. 10. It is observed that hexagonal plate alumina shapes formed for CP powders with particle sizes in the range of 2–500 μm (Fig. 10a). AC powders revealed rice shape particles in which the interaction of a spherical crystal transformed to agglomerate particles in size of 50–200 nm (Fig. 10b). From the above, smaller size is obtained for AC powders. For AH powder, the SEM image shows white and bright appearance spot particles referred to aluminum phosphate or iron phosphate in alumina matrix that appear in hexagonal form as seen in Fig. $10c_1$. The appearance of aluminum phosphate or iron phosphate was confirmed by the EDAX (Fig. $10c_2$) and demonstrated in the XRD and SEM results.

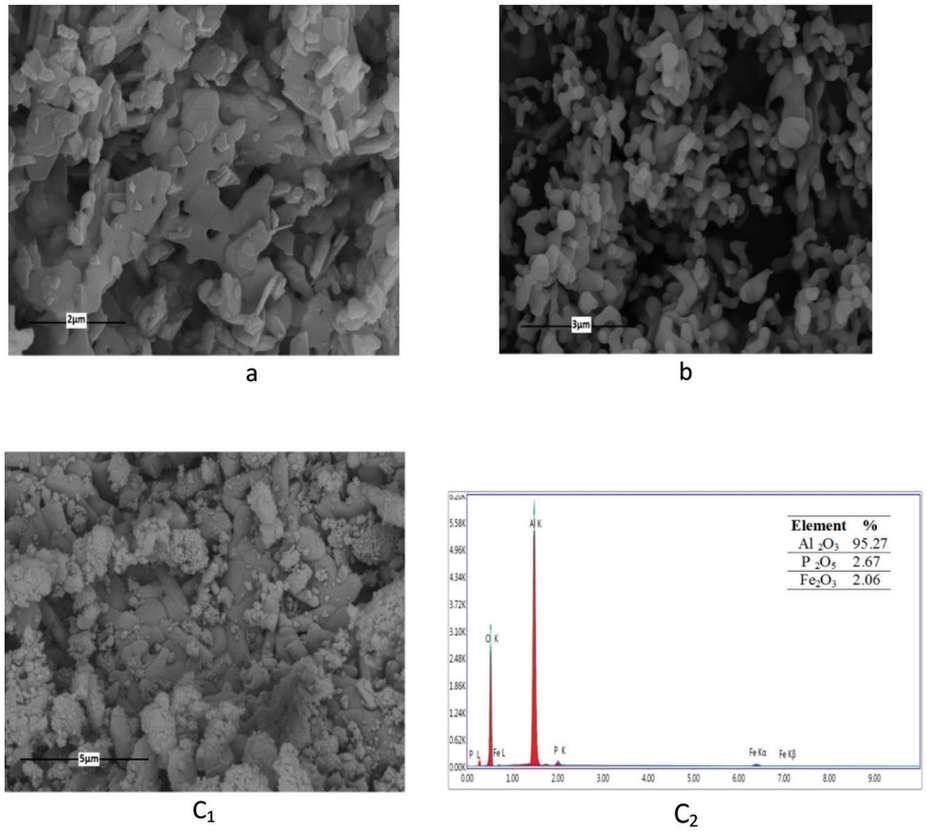

Fig. 10. SEM for the calcined powders; a: CP, b: AC, C_1: AH and C_2: EDAX for AH at 1400°C.

3.2.3. TEM analysis

TEM analysis for CP powder is shown in Fig. 11a. It is found that the particles appear as plated shadow shape. This may be due to the transformation of α-alumina to sodium aluminate at high temperature, which reversed on EDS crystallinity (appeared in nonsymmetrical ring shape). The AH samples (Fig. 11b) show nano-morphology with average particle size ranged between 20 and 40 nm. For AC powder, the alumina appeared in nano-agglomerated particles in size ranged from 1 to 10 nm (Fig. 11c). From the above, the most decreasing sizes were appeared for AC powder.

3.2.4. IR analysis

The FTIR spectra of AC heated at different temperatures: 1000°, 1200° and 1400°C (Fig. 12), show broad band at 3440 cm^{-1} and band at 1635 cm^{-1} assigned to OH stretching and bending vibration. The intensity of these bands decreased with increasing the calcination temperature.

The spectrum of AC calcined at 1000°C shows the signature extending band of the γ-Al_2O_3 in the range 825–522 cm^{-1} [43]. Raising calcination temperature to 1200° and 1400°C shows the characteristic sharp absorption peaks for alpha alumina at 447, 581, 647cm^{-1} and 451, 593, 650 cm^{-1}, respectively. Symmetric bending vibration of Al-O appears at 713, 1046 cm^{-1} and 716, 1055 cm^{-1} for AC calcined at 1200° and 1400°C, respectively [40,43]

Fig. 13 shows the FTIR spectra of CP calcined at different temperatures: 1000°, 1200° and 1400°C. Stretching and bending vibration of OH appear at 3440 and 1635 cm^{-1}. The strong broad band appears at 583–829 cm^{-1} corresponding to Al-O stretching vibration for gamma alumina. By raising the calcination temperature to 1200° and 1400°C γ-alumina converted into α-alumina and sodium aluminate appeared at 1056, 779, 498 cm^{-1} and 1053, 779, 498 cm^{-1} at 1200° and 1400°C, respectively [35].

The FTIR spectra of AH calcined at different temperatures: 1000°, 1200° and 1400°C is shown in Fig. 14. AH powders calcined at 1000°C shows the broad band in the range of 522–825cm^{-1} assigned to γ-Al_2O_3. Also band of organic materials appears at 1458 and 873 cm^{-1} that may be referred to adsorption of organic matter from the sludge on the surface of aluminum hydroxide at this pH (5.5–6). AH powders fired at 1200° and 1400°C show beside alpha alumina bands PO_4^{3-} bands which indicating the presence of phosphate phase together with alpha alumina. The PO_4^{3-} stretching vibration occur at 1024, 1132 cm^{-1} and 1029, 1162 cm^{-1} for AH calcined at 1200° and 1400°C, respectively. However, PO_4^{3-} bending vibration occurs as doublet bands at 450, 496 cm^{-1} and 450, 601 cm^{-1} for AH calcined at 1200° and 1400°C, respectively. Al-O stretching vibration bands of α- Al_2O_3 overlap with the PO_4^{3-} bending vibration bands.

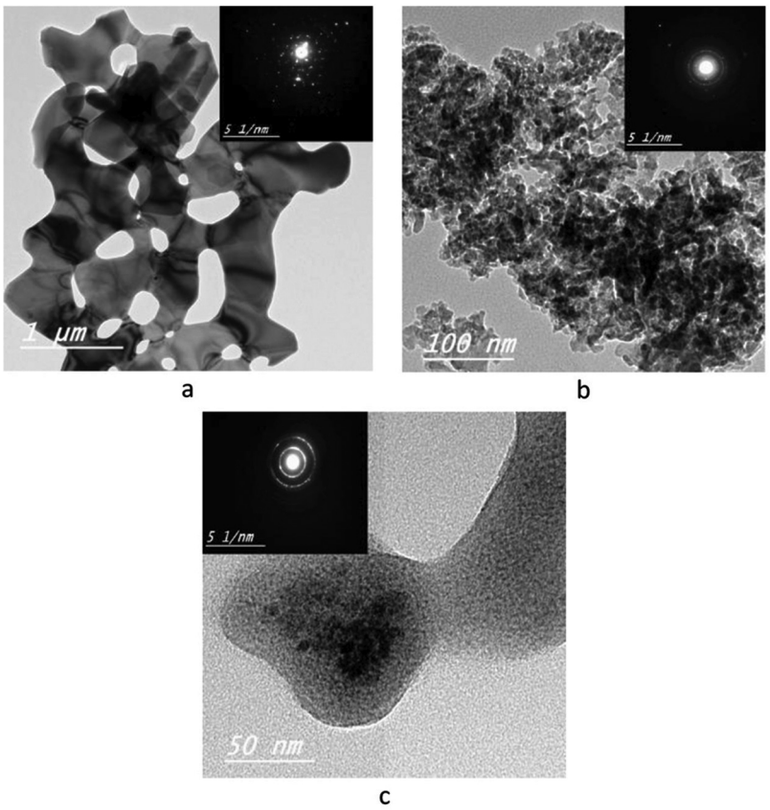

Fig. 11. TEM for the calcined powders CP, AC and AH at 1400°C.

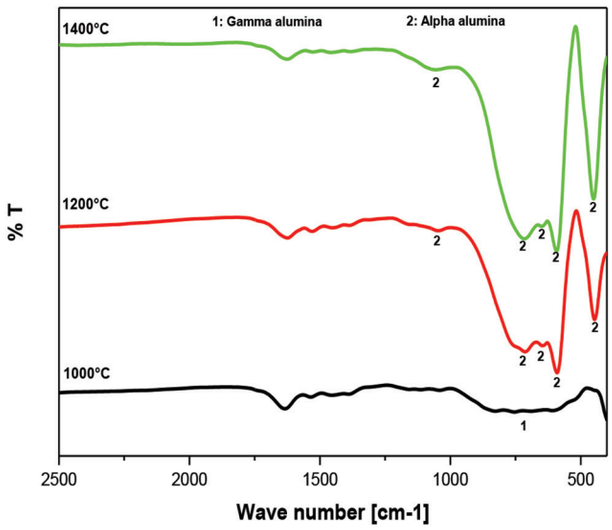

Fig. 12. FTIR spectra of AC calcined at different temperatures.

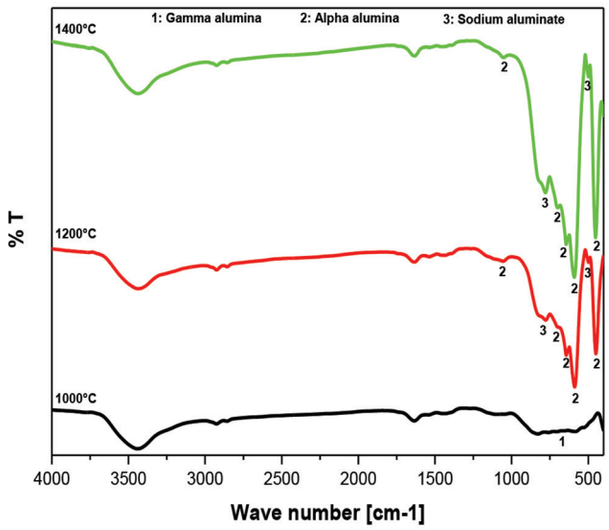

Fig. 13. FTIR spectra of CP calcined at different temperatures.

3.2.5 BET analysis

The BET analysis of the CP, AC and AH powders is shown in Table 3. It is found that the increase of calcination temperatures causes a decrease in the surface area for all powders due to the increasing of particle size. As seen from Table 3, the AC powder shows a high surface area at 1400°C compared with the other powders, which was confirmed by TEM results.

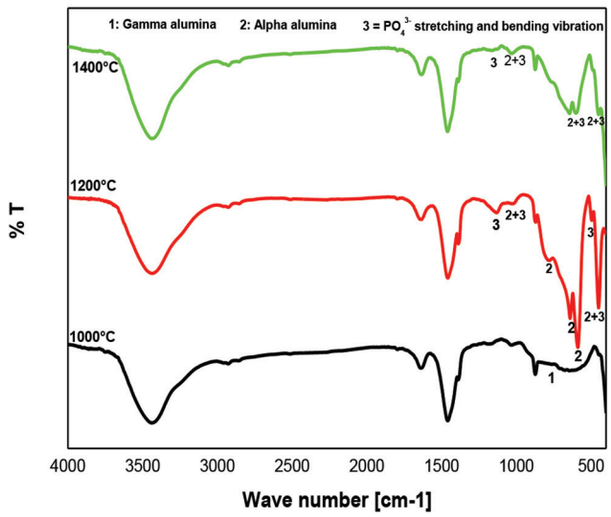

Fig. 14. FTIR spectra of AH calcined at different temperatures.

Table 3
The BET surface area for the CP, AC and AH powders calcined at different temperature

Temp. (°C)	BET measurement (m^2g^{-1})	BET measurement (m^2g^{-1})	BET measurement (m^2g^{-1})
	CP powders	AH powders	AC powders
1000	1.7110 E^{+01}	8.0274 E^{+01}	1.1497 E^{+02}
1200	6.9775 E^{+00}	1.3454 E^{+01}	7.1763 E^{+01}
1400	4.4250 E^{+00}	6.6669 E^{+00}	1.8486 E^{+01}

4. Conclusion

Present work succeeded in preparation of high pure alpha alumina after treatment at 1400°C through recycling of alum sludge which is one of the serious problems that produced as a by-product during water treatment. This work depended on the treatment of alum sludge by different chemical methods to determine the purity of the obtained alpha alumina to produce products that can be entered in many fields based on consuming large amounts of alumina such as furnace lining, ceramics, cement products and pigments. The results indicate that the combination of NaOH and ammonium acetate for alumina preparation is the best method for obtaining high pure alpha alumina in nano size 1–20 nm after heat treatment at 1400°C. The treatment by NH_4OH in one step is the best economic way in lowering the cost of alpha alumina that containing a very small amount of phosphate and iron oxide impurities.

Acknowledgment

The team work thanks the National Research Centre which supports the present work through the project No. 11070203.

References

[1] K.M. Breesem, F.G. Faris, I.M. Abdel-Magid, A general overview: Reuse of alum sludge in construction materials and concrete works, Infrastructure Univ. Kuala Lumpur Res. J., 2 (2014) 20.
[2] Malaysia-Japan economic partnership: Malaysia water services industry and water treatment sludge issues, National water services commission, (SPAN), (2010) 8–14.
[3] P. Verlicchi, L. Masotti, Reuse of drinking water treatment plants sludge in agriculture, Problems-perspective and limitations, Technology transfer. Proceedings of the 9th International Conference on the FAO ESCORENA Network on Recycling of Agricultural, Municipal and Industrial Residues in Agriculture, 9 (2001) 67–73.
[4] R.R. Zamora, C.O. Alfaro, Valorization of drinking water treatment sludge's as raw materials to produce concrete and mortar, J. Environ. Sci., 4(3) (2008) 223–228.
[5] A. Hovsepyan, J.C.J. Bonzongo, Aluminium drinking water treatment residuals (Al-WTRs) as sorbent for mercury, implications for soil remediation, J. Hazard. Mater., 164(1) (2009) 73–80.
[6] Y.F. Zhou, R.J. Haynes, Removal of Pb (II), Cr (II), and Cr (VI) from aqueous solutions using alum-derived water treatment sludge, Water Air Soil Pollut., 215 (2010) 631–643.
[7] G.J. Buglee, C.R. Frink, Alum sludge as soil amendment: Effects on soil properties and plant growth, Conn. Aes. Bull., 827 (1985) 1–8.
[8] L.Y. Wang, D.S. Tong, L.Z. Zhao, F.G. Liu, N. An, W.H. Yu, C.H. Zhou, Utilization of alum sludge for producing aluminum hydroxide and layered double hydroxide, Ceram. Int., 40 (2014) 15503–15514.
[9] Y.F. Maa, L. Zhao, L.G. Payne, D.X. Chen, Stabilization of alum-adjuvanted vaccine dry powder formulations: Mechanism and application, J. Pharm. Sci., 92 (2003) 319–332.
[10] P.K. Singh, P. Kumar, T. Seth, H.W. Rhee, B. Bhattacharya, Preparation, characterization and application of nano-CdS doped with alum composite electrolyte, J. Phys. Chem. Solids, 73 (2012) 1159–1163.
[11] T.W. Martinek, D.L. Klass, Thickened compositions containing a hydrate of an alum, U.S. Patent no. 3,180,827, Patent and Trademark Office, Washing ton, DC, US, (1965).
[12] D.S. Tong, M. Liu, L. Li, C.X. Lin, W.H. Yu, Z.P. Xu, C.H. Zhou, Transformation of alunite residuals into layered double hydroxides and oxides for adsorption of acid red dye, Appl. Clay Sci., 70 (2012) 1–7.
[13] Y. Yang, Y.Q. Zhao, A.O. Babatunde, P. Kearney, Two strategies for phosphorus removal from reject water of municipal waste water treatment plant using alum sludge, Water Sci. Technol., 60 (2009) 3181–3188.
[14] Y.F. Zhou, R.J. Haynes, Removal of Pb (II), Cr (III), and Cr (VI) from aqueous solutions using alum-derived water treatment sludge, Water Air Soil Pollut., 215 (2011) 631–643.
[15] Y.S. Kim, D.H. Kim, J.S. Yang, K. Baek, Adsorption characteristics of As (III) and As (V) on alum sludge from water purification facilities, Sep. Sci. Technol., 47 (2012) 2211–2217.
[16] J. Robertson, The manufacture of aluminium sulfate, i-chemicals for aluminium sulfate-3, available at https://nzic.org.nz/chemprocesses/production/1f.pdf.
[17] A. Boumaza, L. Favaro, J. Ledion, G. Sattonnay, J.B. Brubach, P. Berthet, A.M. Huntz, P. Roy, R. Tetot, Transition alumina phases induced by heat treatment of boehmite: An X-ray diffraction and infrared spectroscopy study, J. Solid State Chem., 182 (2009) 1171–1176.
[18] A.M. Lejus, Formation at high temperature of non-stoichiometric spinels and of derived phases in several oxide systems based on alumina and in the system alumina-aluminum nitride, Hautes Temp. Refract., 1 (1964) 53.
[19] G.W. Lee, Phase transition characteristics of flame-synthesized gamma-Al_2O_3 nanoparticles with heat treatment, Int. J. Chem. Molec. Nucl. Mater. Metal. Eng., 7(9) (2013).
[20] J. Li, Y. Pan, C. Xiang, Q. Ge, J. Guo, Low temperature synthesis of ultrafine α-Al_2O_3 powder by a simple aqueous sol–gel process, Ceram. Int., 32 (2005) 587–591.

[21] M.G. Ma, Y.J. Zhu, Z.L. Xu, A new route to synthesis of γ-alumina nanorods, Mater. Lett., 61 (2007) 1812–1815.
[22] U.Y. Hwang, S.W. Lee, J.W. Lee, H.S. Park, K.K. Koo, S.J. Yoo, H.S. Yoon, Y.R. Kim, Synthesis of porous Al_2O_3 particles by sol-gel method, J. Korean Inst. Chem. Eng., 39 (2001) 206–212.
[23] J.W. Lee, H.S. Yoon, U.S. Chae, H.J. Park, U.Y. Hwang, H.S. Park, D.R. Park, S.J. Yoo, A comparison of structural characterization of composite alumina powder prepared by sol-gel method according to the promoters, Korean Chem. Eng. Res., 43 (2005) 503–510.
[24] H.J. Youn, J.W. Jang, I.T. Kim, K.S. Hong, Low-temperature formation of α-alumina by doping of an alumina-sol, J. Colloid Interface Sci., 211 (1999) 110–113.
[25] Y.K. Park, E.H. Tadd, M. Zubris, R. Tannenbaum, Size-controlled synthesis of alumina nanoparticles from aluminum alkoxides, Mater. Res. Bull., 40 (2005) 1506–1512.
[26] Y. Rozita, R. Brydson, A.J. Scott, An investigation of commercial gamma-Al2O3 nanoparticles, J. Phys. Conf. Ser., 241, Article ID 012096, (2009).
[27] M.G. Ghoniem, T.M. Sami, S.A. El-Reefy, S.A. Mohamed, The production of high purity alumina from solid wastes obtained from aluminium factories, Waste Manage. Environ. VII, 180 (2014) 29–40.
[28] E. Andersson, H. Hansson, Precipitation of reactive aluminium hydroxide from an acidic aluminium sulphate solution by addition of sodium hydroxide, available at http://www.chemeng.lth.se/exjobb/011.pdf.
[29] J. Hoekstra, manufacture of alumina from the reaction of ammonium hydroxide with aluminum sulphate, US patent 3,112,995, (1993).
[30] L. Steven Nail, Structure of aluminum hydroxide gel I: Initial precipitate, J. Pharm. Sci., 65(8) (1976) 1188–1191.
[31] K.A. Matori, L.C. Wah, M. Hashim, I. Ismail, M.H.M. Zaid, Phase transformations of a-alumina made from waste aluminum via a precipitation technique. Int. J. Mol. Sci., 13 (2012) 16812–16821.
[32] J.G. Li, X. Sun, Synthesis and sintering behavior of a nanocrystalline a-alumina powder, Acta. Mater., 48 (2000) 310–312.
[33] M. Ipek, N. Toplan, H.O. Toplan, Transformation kinetics of h- to a-phase of alumina powders prepared from different alumina salts by chemical processing, J. Therm. Anal. Calorim., 125 (2016) 645–649.
[34] P. Palmero, B. Barbara, F. Lomello, E. Garrone, L. Montanaro, Role of the dispersion route on the phase transformation of a nanocrystalline transition alumina, J. Therm. Anal. Calorim., 97 (2009) 223–229.
[35] AZoM, Preparation of sodium aluminate from basic aluminium sulfate, Azojomo, 2 (2006) 1–18.
[36] M. Guo, W. Song, Nutrient value of alum-treated poultry litter for land application, Poult. Sci., 88 (2009) 1782–1792.
[37] M. Ipek, N. Toplan, H.O. Toplan, Transformation kinetics of h- to a-phase of alumina powders prepared from different alumina salts by chemical processing, J. Therm. Anal. Calorim., 125 (2016) 645–649.
[38] A. Eliassi, M. Ranjbar, Application of novel gamma alumina nano structure for preparation of dimethyl ether from methanol, Int. J. Nanosci. Nanotechnol., 10 (2014) 13–26.
[39] S.A. Hosseini, A. Niaei, D. Salar, Production of γ-Al_2O_3 from kaolin. J. Phys. Chem., 1 (2011) 23–27.
[40] K. Djebaili, Z. Mekhalif, A. Boumaza, A. Djelloul, XPS, FTIR, EDX, and XRD analysis of Al_2O_3 scales grown on PM2000 Alloy, J. Spectrosc., 16 (2015) 1–18.
[41] L.Y. Lee, B. Wang, H. Guo, J.Y. Hu, S.L. Ong, Aluminum-based water treatment residue reuse for phosphorus removal, Water, 7 (2015) 1480–1496.
[42] Wisconsin, Department of Natural Resources: Advanced phosphorus removal study guide, (2009) available at dnr.wi.gov/regulations/opcert./WWSGPhosphorusADV.pdf.
[43] J.A. Gadsden, Infrared spectroscopy of mineral and related inorganic compounds, Butterworths, London, (1975) 43.